CORPUS PUBLISHERS

Journal of Mineral and Material Science (JMMS)

ISSN: 2833-3616

Volume 5 Issue 5, 2024

Article Information

Received date : November 23, 2024

Published date: December 18, 2024

*Corresponding author

Freddy H Escobar, Petroleum Engineering Department, Universidad Surcolombiana, Colombia

DOI: 10.54026/JMMS/1099

Key Words

Pressure; Permeability; Flow Regimes; Hydraulic Fractures

Review Article

Beyond Three Dimensions: Decoding Multidimensional Flow Dynamics Through Innovations in Pressure Derivative Slopes for Better Understanding Reservoir Flow Regimes

Freddy H Escobar[1]* and Matilde Montealegre[2]

[1]Universidad Surcolombiana, Petroleum Engineering Department, Colombia

[2]Universidad Surcolombiana, Software Eingeering Department, Colombia

Abstract

Pressure derivative analysis has long been a cornerstone of well-test interpretation, offering invaluable insights into reservoir flow regimes and their associated dimensions. This paper investigates the relationship between the slope of the natural logarithmic pressure derivative and flow dimensions, proposing a novel perspective that extends beyond the conventional three-dimensional space. By analysing key flow regimes such as radial, linear, bilinear, and spherical stabilization flows, the study demonstrates how the concurrent interaction of multiple flow behaviours can exhibit characteristics indicative of higher-dimensional systems. Theoretical derivations for pressure derivatives and equivalent times are presented, facilitating accurate interpretation and mitigating superposition effects during pressure buildup tests. The findings not only enhance diagnostic capabilities but also challenge traditional understandings of fluid dynamics in porous media, providing a groundbreaking framework for reservoir characterization in complex geological settings.

Nomenclature: k: Reservoir Permeability, md; n: Flow Consistency Index; P: Pressure, psi; P': Pressure Derivative, psi; r: Radius , ft; t: Time, days; t_D: Dimensionless Time Coordinate; t_p: Production Time, hr; t_D*P_D': Dimensionless Natura Log Pressure Derivative

Suffices: D: Dimensionless, Dimension; e: Equivalent; eSP_STB: Equivalent Spherical Stabilization; eSP: Equivalent Spherical; eBR: Equivalent Birradial; eBL: Equivalent Bilinear; eL: Equivalent Linear

Introduction

Pressure derivative and deconvolution are indispensable tools in the field of well test interpretation. Although early attempts at their application were made-such as Jones's efforts to use the rate of change of well pressure with time to detect reservoir boundaries-it was [1], and subsequently (Tiab and Kumar, 1980), who formally introduced the pressure derivative function concept. Jones's approach remained numerical, lacking a comprehensive understanding of flow behavior. In contrast, Tiab [1] applied the pressure derivative to the Exponential Integral (Ei) solution of the radial diffusivity equation, leveraging Leibniz's rule to elucidate its behavior during the Infinite-Acting Radial Flow (IARF) regime. This work demonstrated that the pressure derivative forms a straight line under IARF conditions, simplifying the identification of this flow regime compared to the trial-and-error analysis of pressure-versus-time trends. This breakthrough established the pressure derivative as an essential diagnostic tool. Later, (Bourdet et al., 1983) advanced its practical application by introducing the natural logarithmic pressure derivative versus time plot, paving the way for commercial well-test interpretation software.

Tiab, 1995 introduced the TDS (Tiab's Direct Synthesis) technique for interpreting pressure tests, a method heavily reliant on the pressure derivative. In his recent book, [2] consolidates many of his significant contributions to well-test analysis, emphasizing the critical role of the pressure derivative in understanding reservoir dynamics. Additionally, Escobar et al. [3] provides a comprehensive summary of various scenarios where the TDS technique can be effectively applied, highlighting its versatility in reservoir characterization.

The pressure derivative has since enabled the identification of diverse flow regimes. For example, Escobar et al. [4] introduced the parabolic flow regime, characterized by a negative half-slope on the pressure derivative plot. This regime, often referred to as "linear stabilization," appears in elongated reservoirs where a well is off-centered and near a constant-pressure boundary. Sui et al. [5] described it as the dipolar flow regime, while Escobar et al. [6] identified and characterized the spherical stabilization flow regime. These contributions highlight the evolving utility of the pressure derivative in understanding reservoir dynamics. Building on this foundation, Tiab [7] introduced the second pressure derivative concept, which has primarily been used for diagnostic purposes. For instance, Escobar et al. [8] employed the second derivative to estimate distances to discontinuities in areal anisotropic reservoirs. More recently, Tiab [2] extended its application to estimate reservoir permeability in short-duration tests lacking radial flow regimes. His innovative approach provided a unique analytical technique for characterizing reservoirs under phase redistribution conditions.

On a log-log plot of pressure derivative versus time, various flow regimes exhibit distinctive slopes that reveal critical reservoir properties. For instance, during Pseudosteady-State (PSS), the pressure derivative displays a unit slope, indicative of zero flow in the reservoir and zero-dimensional behavior. Linear flow exhibits a half slope, corresponding to one-dimensional flow, while radial flow shows a flat line, representing two-dimensional behavior where flow occurs along both x and y axes. The spherical flow regime, with a negative half slope, represents three-dimensional flow. Each transition in slope corresponds to a change in flow dimensionality, highlighting the geometric complexity of fluid movement within the reservoir.

This paper aims to explore how the combination of multiple flow regimes can transcend conventional three-dimensional interpretations, presenting a conceptual framework for understanding well-test behavior beyond a 3D perspective. By examining the interplay of flow regimes and their diagnostic signatures, this study provides new insights into the multidimensional nature of reservoir characterization. This study is particularly groundbreaking as it bridges the gap between theoretical and practical aspects of reservoir flow analysis. By elucidating the slope dynamics of the pressure derivative, it provides a framework that not only simplifies the analytical characterization of flow regimes but also offers a strategic advantage for defining mathematical models. These insights are pivotal for deciding whether to employ numerical simulation or analytical approaches for reservoir evaluation. This dual application-enhancing analytical clarity and guiding modeling decisions-solidifies the study's relevance, setting a new standard for understanding and applying multidimensional flow dynamics in complex reservoir systems.

Pressure Derivative Function Background

The pressure derivative for a radial infinite reservoir, introduced by Tiab [7], is expressed as:

$$P_D' = \frac{\partial P_D}{\partial t_D} = \frac{1}{2t_D} e^{-\frac{r_D^2}{4t_D}} \quad (1)$$

At the well, r_D=1, Equation (1) simplifies to:

$$P_D' = \frac{\partial P_D}{\partial t_D} = \frac{1}{2t_D} e^{-\frac{1}{4t_D}} \quad (2)$$

Tiab [1] observed that the exponential term in Equation (2) approaches unity for t_D>250, resulting in:

$$P_D' = \frac{1}{2t_D} \quad (3)$$

This indicates that the arithmetic pressure derivative forms a straight line. Applying the natural logarithm to both sides of Equation (3) yields:

$$\log P_D' = -\log t_D - \log 2 \quad (4)$$

Equation (4) describes a negative unit-slope line on a log-log plot of the arithmetic pressure derivative versus time, particularly evident at early times (Figure 1). This plot, initially developed by Tiab [7] and [9] using the superposition principle, also reveals that during the pseudosteady-state period at late times, the slope approaches zero.

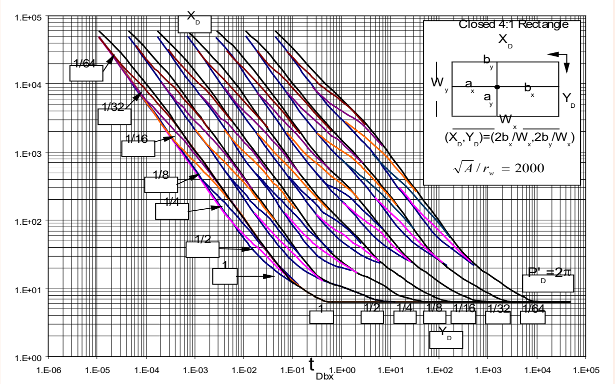

Figure 1: Dimensionless arithmetic pressure derivative versus dimensionless time log-log plot. Taken from [7].

The natural logarithmic pressure derivative is defined as:

$$t_D * P_D' = \frac{1}{2} = \frac{\partial P_D}{\partial \ln t_D} \quad (5)$$

For an off-centered well in a rectangular-shaped reservoir, the dimensionless pressure and natural logarithmic pressure derivative versus time plot is illustrated in Figure 2. Two key advantages emerge when comparing Figures 1 & 2:

a. **Compact visualization:** Figure 2 requires only three log cycles on the y-axis, whereas Figure 1 spans five log cycles.
b. **Radial flow identification:** The flat slope associated with radial flow is easier to identify in Figure 2 compared to the inclined slope in Figure 1.

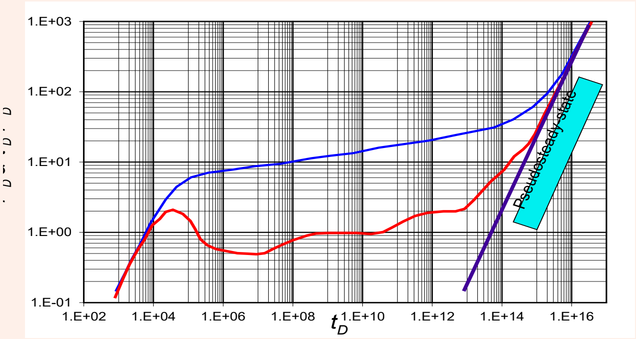

Figure 2: Dimensionless logarithmic pressure derivative versus dimensionless time log-log plot.

The widespread use of natural log pressure derivatives in well test literature stems from these advantages. However, distinct flow regimes can still be characterized by specific pressure derivative functions derived from the natural logarithmic derivative:

Linear pressure derivative:

$$\frac{2(t_D * P_D')}{\sqrt{t_D}} \quad (6)$$

Spherical, hemispherical, parabolic pressure derivative:

$$2(t_D * P_D')\sqrt{t_D} \quad (7)$$

Bilinear pressure derivative:

$$\frac{4(t_D * P_D')}{\sqrt[4]{t_D}} \quad (8)$$

Birradial or elliptical derivative:

$$\frac{25(t_D * P_D')_D}{9\sqrt[25]{t_D^9}} \quad (9)$$

Spherical stabilization pressure derivative:

$$\frac{2(t_D * P_D')}{3\sqrt{t_D^3}} \quad (10)$$

Figure 3 contains Logarithmic pressure derivative and linear pressure derivative versus time comparison. The figure highlights that during the radial flow regime (0.3-11 hours), the logarithmic pressure derivative exhibits a flat slope, whereas during linear flow (13-200 hours), the linear pressure derivative remains flat. The inclusion of the superposition time, t_p, is crucial for accurate pressure derivative estimation. Its omission can produce distorted and meaningless results. Agarwal [10] addressed this by introducing the concept of equivalent time, defined for radial flow as:

$$\Delta t_e = \frac{t_p \Delta t}{\Delta t + t_p} \quad (11)$$

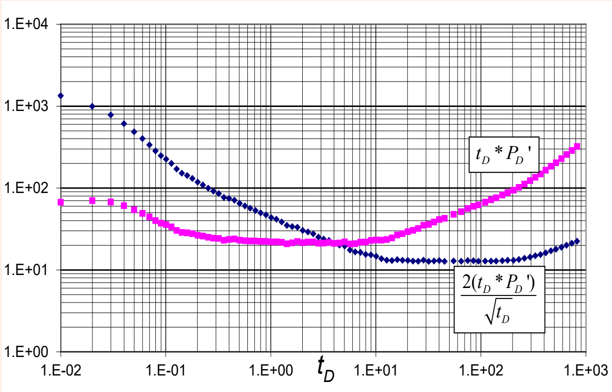

Figure 3: Logarithmic pressure derivative and linear pressure derivative versus time comparison.

Here, some other equivalent times are given for such other flow regimes as:

Linear equivalent time:

$$\Delta t_{eL} = \left[\sqrt{t_p} + \sqrt{\Delta t} - \sqrt{t_p + \Delta t}\right]^2 \quad (12)$$

Bilinear equivalent time

$$\Delta t_{eBL} = \left[\sqrt[4]{t_p} + \sqrt[4]{\Delta t} - \sqrt[4]{t_p + \Delta t}\right]^4 \quad (13)$$

Birradial equivalent time

$$\Delta t_{eBR} = \left[\sqrt[25]{t_p^9} + \sqrt[25]{\Delta t^9} - \sqrt[25]{(t_p + \Delta t)^9}\right]^{25/9} \quad (14)$$

Spherical equivalent time (hemispherical, parabolic)

$$\Delta t_{esP} = \frac{1}{\left[\frac{1}{\sqrt{t_p}} + \frac{1}{\sqrt{\Delta t}} - \frac{1}{\sqrt{t_p + \Delta t}}\right]^2} \quad (15)$$

Spherical stabilization equivalent time

$$\Delta t_{esP\_STB} = \frac{1}{\left[\frac{1}{\sqrt{t_p^3}} + \frac{1}{\sqrt{\Delta t^3}} - \frac{1}{\sqrt{(t_p + \Delta t)^3}}\right]^{2/3}} \quad (16)$$

Effects of Flow Regimes on the Slope of the Natural Logarithmic Pressure Derivative Function

Each flow regime has a unique effect on the slope of the natural logarithmic pressure derivative function, commonly referred to as the "pressure derivative". Among these, the radial flow regime is the most significant in well pressure tests, making the natural log pressure derivative the preferred diagnostic tool in well test analysis.

Flow regime characteristics and dimensionality

Pseudosteady-state (PSS): During the PSS period, the pressure derivative exhibits a unit slope on a log-log plot. This slope forms a 45° angle with the time axis, spanning one log cycle on both axes, as shown in Figure 4. Since no flow occurs within the reservoir, this regime is assigned a dimension (D) of zero.

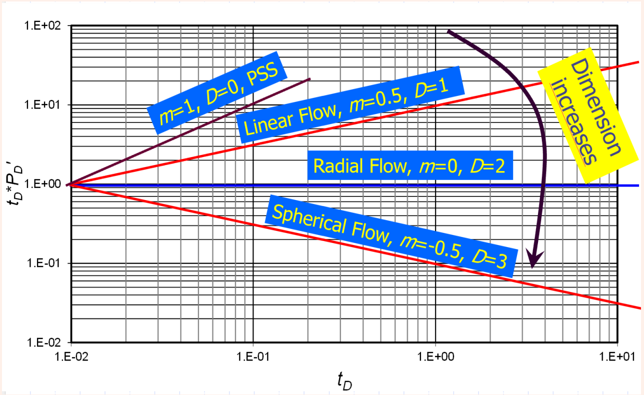

Figure 4: Pressure derivative for most typical flow regime.

Linear flow: Linear flow regimes, such as those occurring in elongated reservoirs or towards hydraulic fractures, exhibit a slope of 0.5. On a log-log plot, the linear flow spans two log cycles on the time axis and one on the derivative axis. This flow regime, associated with unidirectional movement, is assigned a dimension of D=1.

Radial flow: Radial flow displays a zero slope on the pressure derivative curve, corresponding to bidirectional flow in the x and y axes. This two-dimensional flow is characterized by D=2, as illustrated in Figure 4.

Spherical and hemispherical flow: Spherical or hemispherical flow regimes produce a negative half-slope line on the pressure derivative curve. Representing fluid movement in three dimensions, these flows are assigned D=3. Figure 4 shows the increasing dimensionality as the pressure derivative slope decreases in a clockwise manner.

Higher dimensional flow regimes

The interaction of multiple flow regimes within the reservoir can create higher-dimensional flows, as shown in Figures 5 & 6.

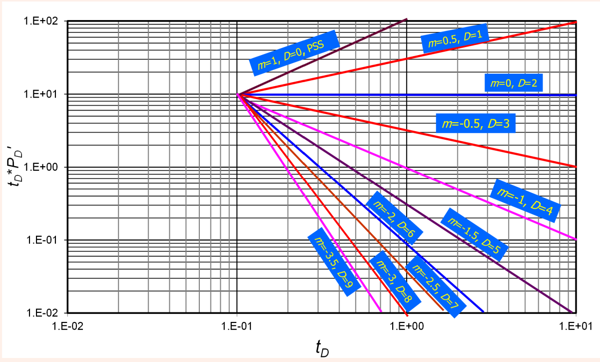

Figure 5: Pressure derivative for dimensions higher than 3.

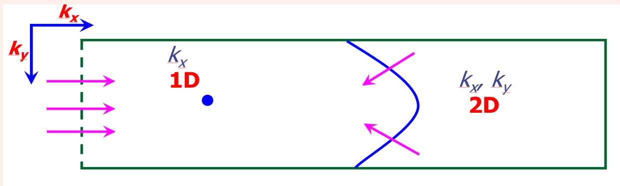

Figure 6: Schematic representation of parabolic flow regime.

Parabolic flow: This regime, introduced by Escobar et al. [4], exhibits a negative half slope identical to that of spherical/hemispherical flow. It arises from simultaneous linear and bidimensional flow within an elongated reservoir near a constant-pressure boundary. Here, a linear piston-like flow (1D) combines with bidimensional flow (2D) along the x and y axes, resulting in an effective dimension of D=3.

Radial stabilization flow: When a constant-pressure boundary exists in an infinite reservoir, the radial stabilization flow regime occurs. Initially, fluid follows a radial flow regime (D=2) until the boundary is reached. At this point, radial flow from the aquifer combines (2D) with reservoir flow, creating a dimension of D=4 and producing a pressure derivative slope of -1, (Figure 7).

Spherical stabilization flow: This flow regime, Escobar et al. [6] characterized by a slope of -1.5 on the pressure derivative curve, represents D=5. It results from concurrent radial flow within the reservoir (D=2) and three-dimensional flow from a gas-cap boundary (D=3). Figure 8 illustrates this combination, which produces a distinct diagnostic feature.

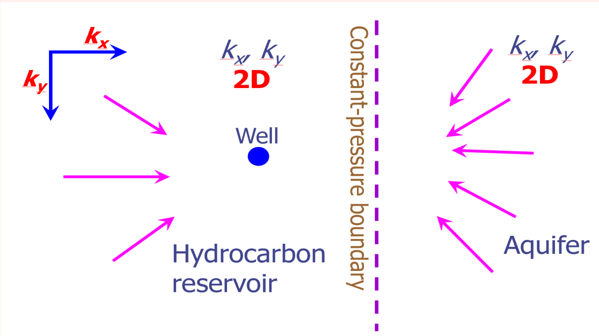

Figure 7: Schematic representation of radial stabilization flow regime.

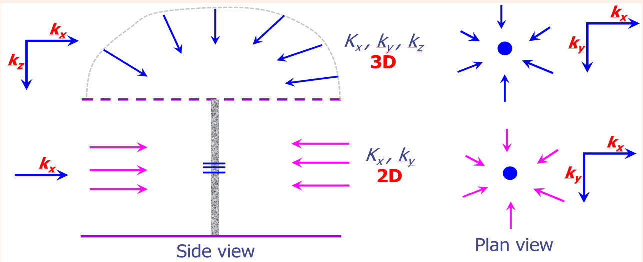

Figure 8: Schematic spherical stabilization flow regime

8D and 9D flow regimes: More complex flow regimes can emerge under certain conditions. For example, a partially completed well in the presence of a gas cap and lower water influx can display a slope of -3 on the pressure derivative curve, corresponding to D=8, (Figure 9). Here, simultaneous 3D flow occurs from the top and bottom boundaries, along with 2D radial flow within the reservoir. If vertical permeability dominates early-time spherical flow, an additional 3D flow may result in D=9, (Figure 10) which corresponds to a partial completion well with open top and bottom boundaries).

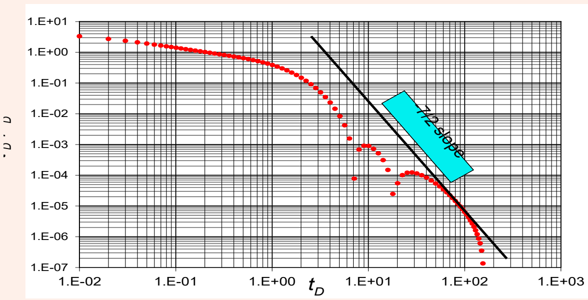

Figure 9: Log-log plot of dimensionless pressure derivative versus time for a flow regime with slope of -7/2.

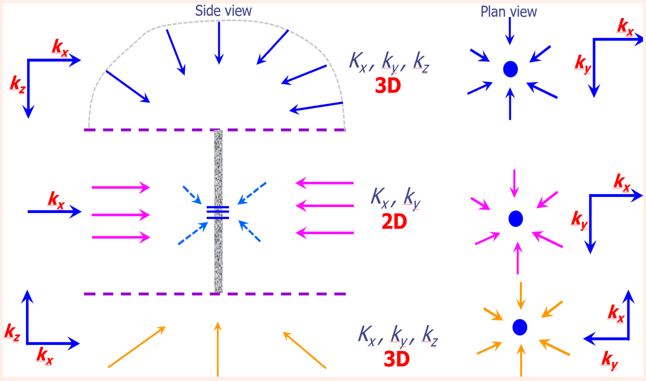

Figure 10: Configuration of 8D and 9D flow regimes.

Specialized flow regimes and slopes, Figure 11

Bilinear and birradial flow: Bilinear flow, occurring in low-conductivity hydraulic fractures or horizontal wells, exhibits a slope of 0.25. Birradial flow, characterized by directional flow emphasis, has a slope of approximately 0.36 (9/25) on the pressure derivative plot. Hese cases are due to the dominance of the flow in a specific dimension.

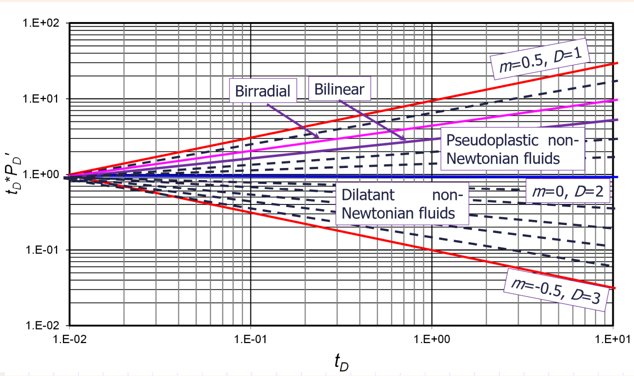

Figure 11: Other pressure derivative slopes found.

Non-Newtonian fluids: In fractal reservoirs or those containing pseudoplastic fluids, derivative slopes [11-14] vary based on the fluid's consistency index (n). For pseudoplastic fluids (n<1), slopes increase from 0 to 0.5, while dilatant fluids (n>1) exhibit slopes decreasing from 0 to -0.5. References to this are many: This behavior is also possible in geothermal reservoirs with dominant outer-region mobility [15]. Both cases, non-Newtonian and geothermal wells occur because the flow has more preference in one direction than the other. Higher slopes, exceeding unity, may be also expected.

Extended scenarios

The practical applications of this approach are particularly relevant in complex systems such as unconventional or geothermal reservoirs, where the interaction between flow regimes and heterogeneous properties is critical. For instance, analyzing pressure derivative slopes can optimize the design of hydraulic fracturing in shale reservoirs, enhancing the estimation of fracture connectivity. Additional applications stemming from this approach include:

Interaction of flow regimes: The superposition of multiple flow regimes can significantly influence fluid dynamics, particularly in cases where reservoir anisotropy generates complex flow patterns. By associating a specific flow dimension with a given scenario, this approach facilitates the identification of boundaries, discontinuities, and heterogeneous structures within the reservoir.

Enhancing practical applications: This methodology is particularly useful in analysing specific scenarios such as unconventional reservoirs (e.g., shale or tight gas), systems with multiple fractures or complex discontinuities, and geothermal reservoirs, where thermal gradients and variable mobility dominate.

For example, consider the scenario depicted in Figure 10, which represents a reservoir with upper and lower constant-pressure boundaries. This configuration results in an eight-dimensional fluid flow regime, as defined by the principles proposed in this paper. This interpretation explains the presence of a -7/2 slope on the pressure derivative curve. Two key benefits arise from such an analysis: (1) the ability to develop either a TDS-based or conventional methodology for well test interpretation, and (2) the capacity to match field data to an appropriate reservoir model for numerical or analytical simulations.

In summary, a synthetic case study of a reservoir with top and bottom open boundaries demonstrated that the combination of two hemispherical flow regimes and a radial flow regime produces fluid behavior resembling an effective dimension of 8D. This insight provides a deeper understanding of pressure derivative slopes and their applications in reservoir characterization.

Conclusion

The slope observed on the log-log plot of the natural logarithmic pressure derivative versus time is strongly correlated with flow dimensions. While constrained by the three-dimensional nature of our physical world, the simultaneous interaction of multiple flow regimes reveals phenomena that suggest higher-dimensional behaviours. This hypothesis is substantiated by the identification and analysis of parabolic, spherical stabilization, and other complex flow regimes. Expressions for estimating pressure derivatives in various flow regimes-including linear, spherical, bilinear, and biradial flows-are presented, alongside equivalent times to mitigate superposition effects during pressure buildup tests. These tools enhance the precision of flow regime identification and reservoir characterization.

The study provides a new framework for interpreting pressure derivative data, emphasizing the need to consider higher-dimensional interactions in complex reservoir systems. Future work should explore the practical implications of these higher-dimensional models in reservoir simulation and well-test optimization, potentially redefining our approach to reservoir engineering. This work lays the groundwork for extending pressure test analysis beyond traditional three-dimensional limits, providing tools to characterize complex systems with greater precision. Future research should focus on integrating these perspectives into numerical simulations and operational strategies, maximizing their practical impact.

This study has redefined the interpretation of pressure derivative slopes by extending the conventional understanding of flow regimes to encompass multidimensional behaviours. The theoretical advancements presented here provide robust tools for analysing flow regimes and their interactions, enabling more precise reservoir characterization. The practical implications are significant, offering enhanced diagnostic capabilities for both analytical and numerical approaches in reservoir engineering. By integrating these novel perspectives into well-test analysis, this work lays a foundation for future research to further explore complex reservoir systems, including unconventional and geothermal reservoirs. Ultimately, these contributions pave the way for more efficient and effective reservoir management strategies, bridging theoretical innovation with practical application.

References

1. Tiab D (1975) A new approach to detect and locate multiple reservoir boundaries by transient well pressure data. N M Tech P 137 MS Thesis.
2. Tiab D (2024) Pressure transient analysis: Pressure derivative. First Ed Elsevier p. 1055.
3. Escobar FH, Jongkittnarukorn K, Hernandez CM (2019) The power of TDS technique for well test interpretation: A short review. J Pet Explor Prod Technol 9: 731-752.
4. Escobar FH, Muñoz O, Sepúlveda J, Montealegre M (2005) New finding on pressure response in long, narrow reservoirs. CTF - Cienc Tecnol Futuro 3: 151-160.
5. Sui W, Mou J, Bi L, Deng J, Economides CE (2007) New flow regimes for well near constant pressure boundary. Presented at the Latin American & Caribbean Petroleum Engineering Conference pp. 15-18.
6. Escobar FH, Ruiz AG, Srivastav P (2015a) Characterization of the spherical stabilization flow regime by transient pressure analysis. ARPN J Eng Appl Sci 10: 5815-5822.
7. Tiab D (1976) Analysis of multiple-sealing faults systems and bounded reservoirs by type-curve matching. PhD Diss, Univ Okla, USA, p. 235.
8. Escobar FH, Bonilla LF, Hernández CM (2018) A practical calculation of the distance to a discontinuity in anisotropic systems from well test interpretation. DYNA Colomb 85: 65-73.
9. Tiab D, Crichlow HB (1979) Pressure analysis of multiple-sealing-fault systems and bounded reservoirs by type-curve matching. Soc Pet Eng J 19(06): 378-392.
10. Agarwal RG (2010) Direct method of estimating average reservoir pressure for flowing oil and gas wells. Presented at the SPE Annual Technical Conference and Exhibition pp. 19-22.
11. Escobar FH, Morela RB, Díaz DS (2020) Characterization of trilinear flow regime in fractal shale reservoirs. ARPN J Eng Appl Sci 15: 1255-1262.
12. Escobar FH, Salcedo LN, Torres CP (2015c) Pressure and pressure derivative analysis for fractal homogeneous reservoirs with power-law fluids. ARPN J Eng Appl Sci 10: 4857-4863.
13. Escobar FH, Morales LL, Gomez KT (2015c) Pressure and pressure derivative analysis for naturally fractured fractal reservoirs. ARPN J Eng Appl Sci 10: 915-923.
14. Escobar FH, Vega LJ, Bonilla LF (2012) Determination of well-drainage area for power-law fluids by transient pressure analysis. CTyF-Cienc Tecnol Futuro 5: 45-56.
15. Horne RN, Satman A, Grant MA (1980) Pressure transient analysis of geothermal wells with phase boundaries. Presented at the SPE Annual Technical Conference and Exhibition pp. 21-24.